


 Cite this: *Chem. Commun.*, 2017, 53, 8866

 Received 27th June 2017,
 Accepted 13th July 2017

DOI: 10.1039/c7cc04958g

rsc.li/chemcomm

Post-synthetic transformation of a Zn(II) polyhedral coordination network into a new supramolecular isomer of HKUST-1†

 Yao Chen,^{ab} Lukasz Wojtas,^c Shengqian Ma,^{id c} Michael J. Zaworotko^{id *d} and Zhenjie Zhang^{id *ea}

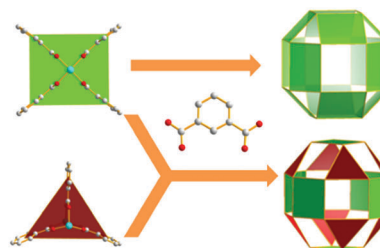
A Zn-based porphyrin containing metal–organic material (porphMOM-1) was transformed into a novel Cu-based porphyrin-encapsulating metal–organic material (porph@HKUST-1-β) via a one-pot post-synthetic modification (PSM) process involving both metal ion exchange and linker installation of trimesic acid. HKUST-1-β is the first example of yao topology and is to our knowledge the first supramolecular isomer of the archetypal coordination network HKUST-1.

Post-synthetic modification (PSM) of metal–organic materials (MOMs), also referred to as metal–organic frameworks, MOFs, or porous coordination polymers, PCPs, is of topical interest because it can afford new materials which might otherwise be difficult or impossible to prepare directly.^{1–8} For example, postsynthetic metal ion^{9–14} and ligand exchange (PSE)^{15–18} generates novel MOMs that are otherwise inaccessible while incorporating functionality such as catalytic sites and/or chirality. Postsynthetic ligand addition (PSA) remains relatively underexplored vs. metal/ligand exchange.^{19–23} Examples of PSA include the following: insertion of a bidentate spacer ligand (4,4'-diazabicyclo[2.2.2]octane) into a 2-D layered MOM to generate a pillared 3-dimensional **pcu** MOM;¹⁹ insertion of a bridging ligand (3,6-di(4-pyridyl)-1,2,4,5-tetrazine) into a 3D MOM, thereby altering gas sorption properties;²⁰ sequential linker installation into multivariate Zr-MOMs with functional groups that are precisely located;²¹ reversible linking of polyhedral cages into 3D nets.²²

Zn(II) MOMs are well-suited for metal ion exchange given the relative lability of d¹⁰ complexes.^{9–14} They also offer diverse

coordination geometries that afford multiple starting points for PSM. For example, Zn(II) can coordinate to three carboxylate ligands to form cationic triangular paddlewheel MBBs, [Zn₂(COO)₃]⁺, or with four carboxylate ligands to form neutral square paddlewheel MBBs, [Zn₂(COO)₄] (Scheme 1, left).^{24–27} This in turn creates diversity in terms of possible MOM structures and topologies as exemplified by the 1,3,5-benzentricarboxylate (btc) based MOMs formed by Zn(II) and Cu(II). Whereas Cu(II) and btc readily form the archetypal **tbo** topology coordination network **HKUST-1**,²⁸ which is based upon regular small rhombihexahedron polyhedral cages sustained by 12 square paddlewheel moieties (Scheme 1, right top). Zn(II) forms two nets based upon regular polyhedral.²⁹ **USF-2**, is isostructural with **HKUST-1**; **USF-1**, is based upon regular small cubicuboctahedron polyhedral cages formed by 6 square paddlewheel moieties and 8 triangular paddlewheel moieties (Scheme 1, right below). A CSD (Cambridge Structural Database)³⁰ survey revealed no entries for [Cu₂(COO)₃]⁺, which suggests that the Cu analog of **USF-1** is unlikely to be readily accessible. In this contribution, we report that a new PSM process involving both PSE and PSA in a one-pot reaction can exploit the lability and structural diversity of a Zn(II) based MOM to generate a novel Cu(II) network that is the first structural isomer of **HKUST-1**.

Reaction of H₃btc, Zn(NO₃)₂ and 5,10,15,20-tetrakis(4-sulfonato-phenyl)porphyrinato iron(III) chloride (FeTPPS) in DMA/H₂O afforded



Scheme 1 Left: Triangle paddlewheel (red) and square paddlewheels (green); right: small rhombihexahedron (up) and small cubicuboctahedron (down).

^a State Key Laboratory of Medicinal Chemical Biology, Nankai University, Tianjin 300071, P. R. China

^b College of Pharmacy, Nankai University, Tianjin 300071, P. R. China

^c Department of Chemistry, University of South Florida, 4202 East Fowler Avenue, Tampa, FL33620, USA

^d Department of Chemistry & Environmental Sciences, Bernal Institute, University of Limerick, Limerick, Republic of Ireland. E-mail: xtal@ul.ie

^e College of Chemistry, Nankai University, Tianjin, 300071, P. R. China.

E-mail: zhangzhenjie@nankai.edu.cn

† Electronic supplementary information (ESI) available. CCDC 1494844 and 1494846. For ESI and crystallographic data in CIF or other electronic format see DOI: 10.1039/c7cc04958g

red-violet prismatic crystals of **porphMOM-1**, $[\text{Zn}_{24}(\text{btc})_{14}(\text{C}_{44}\text{H}_{24}\text{N}_4\text{Fe}(\text{III}))_2(\text{S})]_n$ ($\text{S} = \text{DMA}$ or H_2O). **porphMOM-1** crystallizes in the orthorhombic space group $Pnma$ with $a = 34.304(2)$ Å, $b = 29.205(1)$ Å, $c = 18.774(1)$ Å and $V = 18809(2)$ Å³. UV-Vis spectroscopy confirms the presence of FeTPPS in **porphMOM-1** (Scheme S1 and Fig. S1, ESI[†]) and full loading of FeTPPS was confirmed *via* ICP-MS. A single crystal X-ray diffraction (SCXRD) study revealed that **porphMOM-1** is constructed from three kinds of molecular building blocks (Fig. S2, ESI[†]): $[\text{Zn}_2(\text{COO})_4]$ square paddlewheels; pseudo $[\text{Zn}_2(\text{COO})_4]$ square paddlewheels (Zn is 4-coordinated to three carboxylate moieties and one sulfonate group); $[\text{Zn}_2(\text{COO})_3]^+$ triangular paddlewheels. The average Zn–O bond distance in these building blocks is ~ 1.97 Å, which is consistent with the expected values.³¹ **porphMOM-1** is comprised of three polyhedral cages, the largest of which is an irregular polyhedron that is based upon 6 $[\text{Zn}_2(\text{COO})_4]$ square paddlewheels and 6 $[\text{Zn}_2(\text{COO})_3]^+$ triangular paddlewheels (Fig. 1a and b). The large cage (Fig. S3, ESI[†] and yellow sphere in Fig. 1a) possesses an inner diameter of ~ 12 Å (after subtracting van der Waals radii) and cage windows of ~ 8 Å \times 9 Å. The middle-sized octahemioctahedral cage is formed through linking 8 btc anions by 6 square paddlewheels and 6 triangular paddlewheel MBBs (Fig. 1c, violet cage in Fig. 1a). FeTPPS anions lie in this octahemioctahedral cage and coordinate to the axial sites of 2 square paddlewheels and 2 triangular paddlewheel moieties through their sulfonato moieties. This cage possesses a spherical cavity of a diameter ~ 11 Å and square windows of ~ 8 Å \times 8 Å, which is large enough for small substrates and gas molecules to access the Fe^{3+} centers. In addition, 6 square paddlewheels and 3 triangular paddlewheels are linked by 3 btc anions to generate a small prismatic cage with a triangular window of ~ 5 Å \times 5 Å and a rhombic window of ~ 6 Å \times 9 Å (brown cage in Fig. 1a). By treating btc ligands and triangle paddlewheels as 3-connected nodes, and square paddlewheels as 4-connected nodes, the framework of **porphMOM-1** (trapped porphyrins were omitted) can be described as a 3,3,3,4-connected **tse** net.^{32,33}

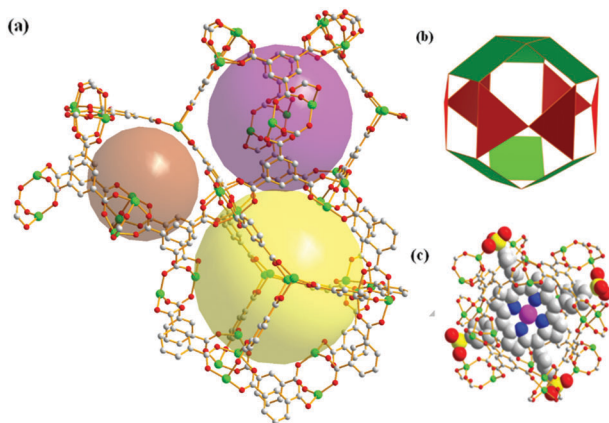
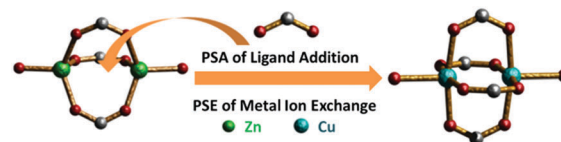


Fig. 1 (a) Three types of polyhedral cages in **porphMOM-1** (large cage filled in yellow, middle cage filled in violet and prism cage filled in brown); (b) large cage comprised of 6 triangular paddlewheel and 6 square paddlewheel moieties; (c) middle cage which contains coordinated FeTPPS moieties (space-filling mode, Zn green, S yellow, N blue, Fe purple).



Scheme 2 A Zn based triangle paddlewheel MBB can transform into a Cu based square paddlewheel MBB via a one-pot PSM process involving PSE of metal ion exchange and PSA of ligand addition.

porphMOM-1 was soaked in MeOH for 10 days and then activated under vacuum. MOMs that are sustained by $[\text{Zn}_2(\text{COO})_3]^+$ MBBs are generally unstable after removal of solvent,^{24–26} so it is unsurprising that no N_2 uptake was observed for activated **porphMOM-1**. Crystals of **porphMOM-1** were subjected to metal ion exchange with Cu^{2+} cations in order to determine if this would enhance structural and hydrolytic stability.³¹ **porphMOM-1** crystals were immersed into 0.04 M $\text{Cu}(\text{NO}_3)_2$ methanol solution for 10 days with refreshment of the solution each day. ICP-MS analysis revealed that only 17% of Zn atoms had been exchanged by Cu. This might be a consequence of the $[\text{Zn}_2(\text{COO})_3]^+$ moieties being unsuitable for exchange with Cu. We considered that structural and charge balance considerations might enable the $[\text{Zn}_2(\text{COO})_3]^+$ MBBs to transform into $[\text{M}_2(\text{COO})_4]$ MBBs by installation of an additional carboxylate moiety (Scheme 2). Moreover, the internal space of the polyhedral cages in **porphMOM-1** are large enough to accommodate guest molecules such as btc (dimensions: ~ 7 Å \times 8 Å). We therefore attempted a new PSM approach based upon combining PSE and PSA in one pot. Thus, **porphMOM-1** crystals were immersed in a MeOH solution of 0.04 M $\text{Cu}(\text{NO}_3)_2$ and 0.0005 M 1,3,5- H_3btc for 10 days with refreshment of the solution every day. ICP-MS analysis of the bulk sample determined that 75% of the Zn cations had been replaced by Cu. SCXRD subsequently revealed that **porphMOM-1** had transformed to a new crystalline phase (**porph@HKUST-1- β**), $[\text{Cu}_{12}(1,3,5\text{-btc})_8(\text{C}_{44}\text{H}_{24}\text{N}_4\text{Fe}(\text{III}))_2(\text{S})]_n$, with unit cell parameters ($a = 18.510(5)$ Å, $b = 18.510(5)$ Å and $c = 30.287(8)$ Å, $V = 8987(4)$ Å³) in the hexagonal space group $P63/mmc$. Notably, **porph@HKUST-1- β** could not be directly synthesized (1,3,5- H_3btc , $\text{Cu}(\text{NO}_3)_2$, FeTPPS, MeOH, room temperature). We observed that **porph@HKUST-1- β** retains the prismatic morphology of its parent, **porphMOM-1**, indicative of a single-crystal-to-single-crystal transformation (Fig. S4, ESI[†]).¹⁴ SCXRD revealed that the three Zn MBBs in **porphMOM-1** had each transformed to $[\text{Cu}_2(\text{COO})_4]$ paddlewheel MBBs. Cu–O(carboxylate) bonds in **porph@HKUST-1- β** exhibit average lengths of ~ 1.945 Å, which is consistent with the values seen in other copper paddlewheel MOMs such as **HKUST-1**.²⁸ Along the same lines, Cu–Cu distances (2.753 and 2.785 Å) are much shorter than the Zn–Zn distances (3.235, 3.445, 3.806 and 2.988 Å) in **porphMOM-1**. UV-Vis spectroscopy confirmed that FeTPPS retained its $\text{Fe}(\text{III})$ centers (Fig. S1, ESI[†]). As revealed by Scheme 2, metal exchange in **porphMOM-1** was accompanied by insertion of carboxylate moieties from btc anions to afford $[\text{Cu}_2(\text{COO})_4]$ MBBs (inserted btc ligands are highlighted in space-filling mode in Fig. S3, ESI[†]). PSM thereby afforded a polyhedral-based framework with unprecedented topology. The additional btc anions in effect convert the triangular paddlewheels in the

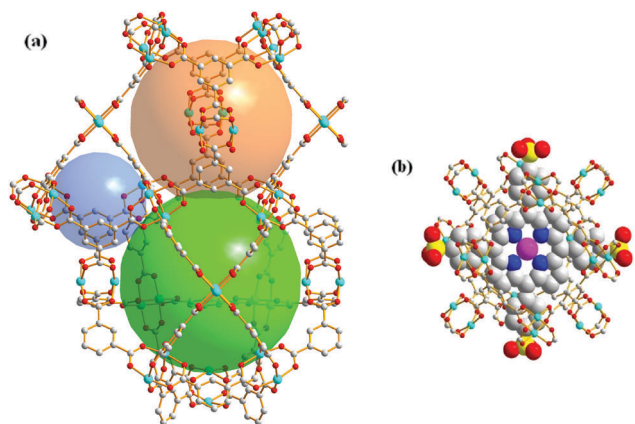


Fig. 2 (a) Three types of polyhedral cages exist in **porph@HKUST-1-β** (nanoball-2, green, octahemioctahedral cage, orange and tetrahedral cage, blue); (b) octahemioctahedral cage with encapsulated FeTPPS moieties. FeTPPS moieties are highlighted in space-filling mode (Cu cyan, S yellow, N blue, Fe purple).

largest cage of **porphMOM-1** (Fig. 1b and Fig. S3, ESI[†]) into square paddlewheels, thereby generating an irregular polyhedral cage with the same connectivity as nanoball-2, first reported by us in 2001 (green cage in Fig. 2a).³⁴ The additional btc anions mean that the prismatic cages (Fig. S3, ESI[†]) are joined to two adjacent tetrahedral cages. The framework of **porph@HKUST-1-β** can be regarded as a new supramolecular isomer of **HKUST-1** (3,4-connected **tbo** net) with 3,3,3,4,4 connectivity (point symbol: $\{6^2 \cdot 8^2 \cdot 10^2\}_3 \{6^2 \cdot 8^3 \cdot 10\}_3 \{6^3\}_7 \{8^3\}$) (Fig. S5, ESI[†]). This new net has been entered into the RCSR database as 'yao'. To clarify the difference between **HKUST-1** and **porph@HKUST-1-β**, the two frameworks are compared side by side in Fig. S6 (ESI[†]). The **tbo** topology network of **HKUST-1** is comprised of three distinct polyhedral cages with stoichiometry 1:1:2: nanoball-1 (also referred to as a small rhombihexahedron or MOP-1),³⁵ an octahemioctahedral cage and a tetrahedral cage. **porph@HKUST-1-β** can also be disassembled into three distinct polyhedral cages: nanoball-2, an octahemioctahedral cage and a tetrahedral cage, with stoichiometry of 1:1:2. nanoball-1 and nanoball-2, the large cavities, and their manner in which they are packed are what distinguish these two Cu-btc polymorphs. Specifically, in **tbo** the large cavities exhibit cubic close packing, whereas in **yao** they exhibit hexagonal close packing. Fig. S7 (ESI[†]) compares nanoball-1 and nanoball-2 and shows that they result from different connectivity of 12 copper square paddlewheels and 24 1,3-bdc (benzene-1,3-dicarboxylate) moieties. In 2001, we reported the existence of nanoball-1 and nanoball-2 as discrete cages and suggested that nanoball-2 would have the potential to serve as a supramolecular building blocks (SBB) to build 3D MOMs.³⁴ **porph@HKUST-1-β** is to our knowledge the first example of such a network. The existence of both nanoball-1 and nanoball-2 can be ascribed to the "partial flexibility" of 1,3-bdc moieties which can sustain twist angles of 0–90° or bend angles of up to 29.7° (Fig. S8, ESI[†]).³⁶ In addition, as revealed by SCXRD, FeTPPS anions are no longer coordinated and revert to being encapsulated in the octahemioctahedral cages (Fig. 2b) of

porph@HKUST-1-β. This type of porphyrin encapsulation was seen in **FeTPPS@HKUST-1** and has been observed in other **porph@MOMs**.^{37–39} It should be noted that FeTPPS can only be encapsulated in the octahemioctahedral cages because the size and symmetry of porphyrins perfectly fit the octahemioctahedral cages but not the large nanoball-2 cage and small tetrahedral cage.³⁷

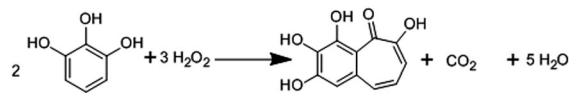
As anticipated, permanent porosity is exhibited by **porph@HKUST-1-β** (Fig. S9, ESI[†]). N₂ sorption revealed that **porph@HKUST-1-β** adsorbs 241 cm³ g⁻¹ of N₂ at 77 K and 1 bar, corresponding to a Langmuir surface area of 731 m² g⁻¹ (BET surface area: 705 m² g⁻¹). In contrast, **porphMOM-1** is non-porous after activation (Fig. S9, ESI[†]), possibly due to the instability of triangular Zn MBBs.^{24–26} Thermogravimetric analysis (TGA) revealed that methanol-exchanged **porphMOM-1** and **porph@HKUST-1-β** undergo weight losses of ~10% and 12%, respectively, below 100 °C, but that they are thermally stable to ~260 °C and 340 °C, respectively (Fig. S10, ESI[†]). The enhanced thermal stability and permanent porosity of **porph@HKUST-1-β** is presumably due to the transformation of the triangular Zn MBBs into [Cu₂(COO)₄] MBBs⁴⁰ and the additional connectivity of the network.

Encapsulated Fe-porphyrin centers have the potential to enable heterogeneous catalysis by serving as catalytically active sites that mimic enzymatic heme centers (*e.g.* peroxidative oxygen transfer).⁴¹ Polyphenols are routinely used for the evaluation of the peroxidase activity of heme-based enzymes. Therefore, 1,2,3-trihydroxybenzene (THB) (dimensions: ~5.7 Å × 5.8 Å) was selected to evaluate the catalytic performance of **porphMOM-1** and **porph@HKUST-1-β** by monitoring the oxidation of THB to the purpurogallin dimer product at 420 nm in acetonitrile ($\epsilon = 4.32 \text{ mM}^{-1} \text{ cm}^{-1}$) at room temperature.⁴²

The results of the catalytic studies are presented in Table 1 and Fig. S11, ESI[†]. They reveal that both **porph@HKUST-1-β** and **porphMOM-1** exhibit fast initial rates of $2.77 \times 10^{-4} \text{ mM s}^{-1}$ and $1.90 \times 10^{-4} \text{ mM s}^{-1}$ respectively, which are comparable to the homogeneous **FeTPPS** system ($6.42 \times 10^{-4} \text{ mM s}^{-1}$). In contrast, the initial rate exhibited by homogeneous **Hemin** is more than 10 times slower than **porph@HKUST-1-β** whereas **HKUST-1** reacts ~5 times slower with a rate of $5.37 \times 10^{-5} \text{ mM s}^{-1}$. This suggests that catalytic activity can be attributed to the FeTPPS in the framework rather than the Cu paddlewheels given that THB is small enough to diffuse into the porphyrin-containing cages.

Table 1 Catalytic oxidation of THB in the presence of 30 mM H₂O₂ in acetonitrile

Catalysts	Initial rate (mM s ⁻¹)	Conversion (%) (72 h)
FeTPPS	6.42×10^{-4}	30.4
porph@HKUST-1-β	2.77×10^{-4}	14.4
porphMOM-1	1.90×10^{-4}	11.5
FeTPPS@HKUST-1	7.81×10^{-5}	4.5
HKUST-1	5.37×10^{-5}	3.1
Hemin	2.74×10^{-5}	8.9
Blank	5.81×10^{-7}	<1



In addition, both **porph@HKUST-1-β** and **porphMOM-1** exhibit higher conversion than reported for **FeTPPS@HKUST-1**. **porph@HKUST-1-β** was chosen as a representative heterogeneous catalyst. The filtrate of **porph@HKUST-1-β** after catalysis did not exhibit the characteristic UV-Vis peak of FeTPPS (Fig. S1, ESI[†]), indicating that no leaching of FeTPPS had occurred during catalysis. Moreover, recyclability data revealed that **porph@HKUST-1-β** can be reused for at least four cycles without significant decrease of catalysis activity and loss of its crystallinity (Fig. S12 and S13, ESI[†]).

In summary, we report herein a new PSM strategy that involves postsynthetic metal ion exchange and ligand addition in a one-pot process. A porphyrin linked MOM (**porphMOM-1**) thereby transforms into a porphyrin-encapsulating MOM (**porph@HKUST-1-β**) in single-crystal to single-crystal fashion. Notably, **HKUST-1-β** is the first example of a supramolecular isomer of the archetypal coordination network **HKUST-1** and results from its 12 square paddlewheels forming an irregular polyhedral cage that is distinct from the regular polyhedral cage observed in **HKUST-1**. **porph@HKUST-1-β** was found to exhibit enhanced stability, permanent porosity and biomimetic catalytic activity towards oxidation of a polyphenol than **porphMOM-1**. This new PSE/PSA strategy enriches the toolbox of PSM strategies and enables the synthesis of a functional porous material that would otherwise be difficult or impossible to achieve. Further, the concerted metal exchange/ligand installation process is unlikely to be limited to the specific case in question. Indeed, it should be general for MOFs that are sustained by labile transition metals such as Zn(II) and Cd(II).

The data for **porphMOM-1** was collected at the Advanced Photon Source on beamline 15ID-C of ChemMatCARS Sector 15, which is principally supported by the National Science Foundation/Department of Energy under grant number NSF/CHE-0822838. The Advanced Photon Source is supported by the U. S. Department of Energy, Office of Science, Office of Basic Energy Sciences, under Contract No. DE-AC02-06CH11357. ZZ acknowledges the China Young 1000 Talents program and NSFC No. 21601093. MZ acknowledges the generous financial support of the Science Foundation Ireland (Grant 13/RP/B2549). We thank Prof. Peng Cheng and Prof. Wei Shi from Nankai University for their assistance in measurement of ICP-MS.

Notes and references

- S. Cohen, *Chem. Rev.*, 2012, **112**, 970.
- S. R. Batten, S. M. Neville and D. R. Turner, *Coordination Polymers: Design, Analysis and Application*, Royal Society of Chemistry, Cambridge, UK, 2009.
- L. R. MacGillivray, *Metal–Organic Frameworks: Design and Application*, John Wiley & Sons, Hoboken, New Jersey, 2010.
- Z. Zhang, W.-Y. Gao, L. Wojtas, S. Ma, M. Eddaoudi and M. J. Zaworotko, *Angew. Chem., Int. Ed.*, 2012, **51**, 9330.
- K. L. Mulfort, O. K. Farha, C. L. Stern, A. A. Sarjeant and J. T. Hupp, *J. Am. Chem. Soc.*, 2009, **131**, 3866.
- A. Shultz, A. Sarjeant, O. Farha, J. Hupp and S. Nguyen, *J. Am. Chem. Soc.*, 2011, **133**, 13252.
- S. Yuan, Y.-K. Deng and D. Sun, *Chem. – Eur. J.*, 2014, **20**, 10093.
- S. Yuan, Y.-K. Deng, W.-M. Xuan, X.-P. Wang, S.-N. Wang, J.-M. Dou and D. Sun, *CrystEngComm*, 2014, **16**, 3829.
- M. Dincă and J. R. Long, *J. Am. Chem. Soc.*, 2007, **129**, 11172.
- T. K. Prasad, D. H. Hong and M. P. Suh, *Chem. – Eur. J.*, 2010, **16**, 14043.
- J. Zhao, L. Mi, J. Hu, H. Hou and Y. Fan, *J. Am. Chem. Soc.*, 2008, **130**, 15222.
- M. Lalonde, W. Bury, O. Karagiari, Z. Brown, J. T. Hupp and O. K. Farha, *J. Mater. Chem. A*, 2013, **1**, 5453.
- C. K. Brozek and M. Dincă, *Chem. Sci.*, 2012, **3**, 2110.
- M. Kim, J. F. Cahill, H. Fei, K. A. Prather and S. M. Cohen, *J. Am. Chem. Soc.*, 2012, **134**, 18082.
- M. Kondo, S. Furukawa, K. Hirai and S. Kitagawa, *Angew. Chem., Int. Ed.*, 2010, **49**, 5327.
- B. J. Burnett, P. M. Barron, C. Hu and W. Choe, *J. Am. Chem. Soc.*, 2011, **133**, 9984.
- O. Karagiari, M. B. Lalonde, W. Bury, A. A. Sarjeant, O. K. Farha and J. T. Hupp, *J. Am. Chem. Soc.*, 2012, **134**, 18790.
- T. Li, M. T. Kozłowski, E. A. Doud, M. N. Blakely and N. L. Rosi, *J. Am. Chem. Soc.*, 2013, **135**, 11688.
- R. Kitaura, F. Iwahori, R. Matsuda, S. Kitagawa, Y. Kubota, M. Takata and T. C. Kobayashi, *Inorg. Chem.*, 2004, **43**, 6522.
- H. J. Park, Y. E. Cheon and M. P. Suh, *Chem. – Eur. J.*, 2010, **16**, 11662.
- S. Yuan, W. Lu, Y.-P. Chen, Q. Zhang, T.-F. Liu, D. Feng, X. Wang, J. Qin and H.-C. Zhou, *J. Am. Chem. Soc.*, 2015, **137**, 3177.
- J.-R. Li, D. J. Timmons and H.-C. Zhou, *J. Am. Chem. Soc.*, 2009, **131**, 6368.
- Z. Chen, S. Xiang, D. Zhao and B. Chen, *Cryst. Growth Des.*, 2009, **9**, 5293.
- Z.-J. Zhang, W. Shi, Z. Niu, H.-H. Li, B. Zhao, P. Cheng, D.-Z. Liao and S.-P. Yan, *Chem. Commun.*, 2011, **47**, 6425.
- X.-R. Hao, X.-L. Wang, K.-Z. Shao, G.-S. Yang, Z.-M. Su and G. Yuan, *CrystEngComm*, 2012, **14**, 5596.
- H. Ma, S. Wang, H. Liu, F. Meng, W. Zheng and W. Gao, *CrystEngComm*, 2015, **17**, 1001.
- D. Kim, X. Liu, M. Oh, X. Song, Y. Zou, D. Singh, K. S. Kim and M. S. Lah, *CrystEngComm*, 2014, **16**, 6391.
- S. S. Chui, S. M. Lo, J. P. Charmant, A. G. Orpen and I. D. Williams, *Science*, 1999, **283**, 1148.
- J. Lu, A. Mondal, B. Moulton and M. J. Zaworotko, *Angew. Chem., Int. Ed.*, 2001, **113**, 2171.
- F. Allen, *Acta Crystallogr., Sect. B: Struct. Sci.*, 2002, **58**, 380.
- M. K. Bhunia, J. T. Hughes, J. C. Fettinger and A. Navrotsky, *Langmuir*, 2013, **29**, 8140.
- M. O'Keeffe and O. M. Yaghi, *Chem. Rev.*, 2012, **112**, 2.
- M. O'Keeffe, M. A. Peskov, S. Ramsden and O. M. Yaghi, *Acc. Chem. Res.*, 2008, **41**, 12.
- B. Moulton, J. J. Lu, A. Mondal and M. J. Zaworotko, *Chem. Commun.*, 2001, 863.
- M. Eddaoudi, J. Kim, J. B. Wachter, H. K. Chae, M. O'Keeffe and O. M. Yaghi, *J. Am. Chem. Soc.*, 2001, **123**, 4368.
- Z. Zhang, L. Wojtas and M. J. Zaworotko, *Cryst. Growth Des.*, 2011, **11**, 1441.
- Z. Zhang, L. Zhang, L. Wojtas, M. Eddaoudi and M. J. Zaworotko, *J. Am. Chem. Soc.*, 2012, **134**, 928.
- R. W. Larsen, L. Wojtas, J. Perman, R. L. Musselman, M. J. Zaworotko and C. M. Vetromile, *J. Am. Chem. Soc.*, 2011, **133**, 10356.
- R. W. Larsen, J. Miksovská, R. L. Musselman and L. Wojtas, *J. Phys. Chem. A*, 2011, **115**, 11519.
- Z. Wei, W. Lu, H.-L. Jiang and H.-C. Zhou, *Inorg. Chem.*, 2013, **52**, 1164.
- Y. Chen, T. Hoang and S. Ma, *Inorg. Chem.*, 2012, **51**, 12600.
- Q. Wang, Z. Yang, L. Wang, M. Ma and B. Xu, *Chem. Commun.*, 2007, 1032.